

## THE DEGRADATION TEST OF IBS (INJECTABLE BONE SUBSTITUTES) PASTE SCAFFOLD USING EIS (ELECTRICAL IMPEDANCE SPECTROSCOPY) METHODS

Inas Amira<sup>a</sup>, Dyah Hikmawati<sup>b</sup>, Kamilia<sup>b</sup>, Khusnul Ain<sup>c</sup>, Ade Agung Harnawan<sup>d</sup>, Bayu Ariwanto<sup>a</sup>, Inten Firdausi Wardhani<sup>c</sup>, Suprijanto<sup>e</sup>, Sari Ayu Wulandari<sup>f</sup>, Hesty Susanti<sup>g</sup>, Andi Besse Firdausiah Mansur<sup>h</sup>, Ahmad Hoirul Basori<sup>h</sup>

<sup>a</sup>Magister of Biomedical Engineering, Airlangga University, Surabaya, Indonesia

<sup>b</sup>Physics, Airlangga University, Surabaya, Indonesia

<sup>c</sup>Biomedical Engineering, Airlangga University, Surabaya, Indonesia

<sup>d</sup>Physics, Lambung Mangkurat University, Banjarmasin, Indoensia

<sup>e</sup>Engineering Physics, Institute Technology Bandung, Bandung, Indoensia

<sup>f</sup>Biomedical Engineering, Dian Nuswantoro University, Semarang, Indonesia

<sup>g</sup>Biomedical Engineering, Telkom University, Bandung, Indonesia

<sup>h</sup>Faculty of Computing and Information Technology in Rabigh, King Abdulaziz University, Rabigh 21911, Saudi Arabia

### Article history

Received

29 October 2024

Received in revised form

7 April 2025

Accepted

10 April 2025

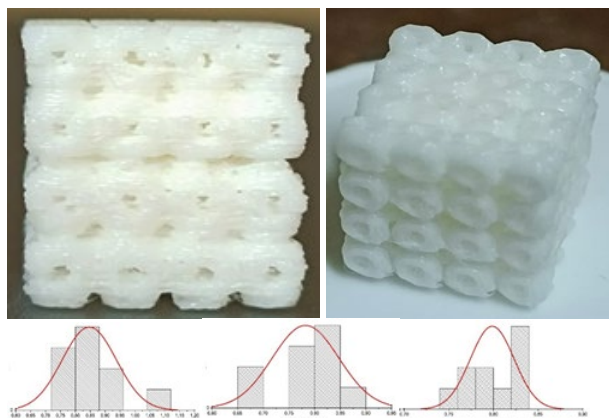
Published Online

23 December 2025

\*Corresponding author  
k\_ain@fst.unair.ac.id

r

### Graphical abstract



### Abstract

There numerous cases of bone tuberculosis requiring immediate treatment. One treatment approach involves local drug delivery using injectable bone substitute (IBS) paste containing streptomycin, combined with monitoring of drug degradation. Although various degradation tests are commonly used, real-time monitoring of IBS weight change and mass loss still requires investigation. This study investigates material degradation and drug release using electrical impedance spectroscopy (EIS) and compares the results with ultraviolet-visible (UV-Vis) analysis. Degradation tests were conducted on five polylactic acid (PLA) scaffold samples with a pore size of 800  $\mu\text{m}$  that were injected with IBS paste and immersed for different durations. The IBS paste was synthesized using a hydroxyapatite-to-gelatin ratio of 65:45 and subsequently injected into the scaffolds, followed by degradation testing over a five-week period. Characterization methods included microscopic observation, degradation evaluation of the IBS paste-infused scaffolds, UV-Vis analysis, and EIS measurements. Microscopic analysis showed that pore sizes ranged from 782.30–805.00  $\mu\text{m}$  before IBS paste injection and decreased to 148.00–189.00  $\mu\text{m}$  after injection. Degradation testing demonstrated that mass reduction of the IBS paste-infused scaffolds increased with immersion time. UV-Vis analysis indicated an upward trend in IBS

paste concentration from 1st week until 5th week, increasing from 1.168% to 2.522%. A five-week release is considered sufficient to support the early stages of bone healing and graft integration. EIS measurements after degradation showed that a parallel RC circuit model correlated with the experimental data, with  $R^2$  values of 0.9325 for resistance and 0.4511 for capacitance.

**Keywords:** Injectable Bone Substitute, paste scaffold, Electrical Impedance Spectroscopy, Degradation test

© 2026 Penerbit UTM Press. All rights reserved

## 1.0 INTRODUCTION

Tuberculosis (TB) is a contagious disease and one of the leading causes of poor health globally, second only to the coronavirus pandemic [1]. In Indonesia, the Ministry of Health reported 700,000 TB cases in 2022, with most patients being of productive age, especially between 45 and 54 years old. Early detection and comprehensive treatment are essential to controlling the spread of TB [2].

Typically, tuberculosis bacteria infect the lungs, but numerous cases have demonstrated its ability to affect other organs, including the spine [3]. Spinal tuberculosis infections can result in damage to the nervous system and the spine itself [4], [5]. This spinal bone damage can lead to deformities, causing the back to protrude [4]. Prevention involves cleaning infected bone tissue and replacing it with bone implants [6], [7].

Bone scaffolds, serving as carriers for bone cells and frameworks, provide space for bone cells to proliferate, differentiate, receive nutrients, and metabolize before new bone cells are formed [8]. Artificial bone scaffolds must balance structural integrity, biological compatibility, and degradability to effectively support bone regeneration [28]. Specifically, in terms of engineering view, there are two main requirements for engineering artificial bone scaffolds: structure and properties [9]. Structurally, bone scaffolds must have a personalized external shape to fit the location of bone defects and interconnected porous structures to facilitate the growth of bone tissue and blood vessels within the structure [10]. In terms of properties, they must possess good mechanical properties to provide structural support and good biological properties to induce bone tissue regeneration [11].

Injectable Bone Substitute (IBS) is a highly biodegradable composite material based on hydroxyapatite-gelatin used as a bone substitute [12], [13]. The advantages of IBS include its ability to be molded to fit the bone cavity which needs to be filled and ability to polymerize after the injection [14]. IBS can harden within 4-8 hours, has viscosity suitable for injection, and has a near-neutral pH when in suspension [12], [15], [16]. Therefore, IBS have important role in drug delivery inside bone.

IBS materials need to be tested for degradation time when they are used on bone. Therefore, degradation testing is performed on IBS samples in Simulated Body Fluid (SBF) [17]. SBF is a solution with a composition and ion concentration nearly equivalent to human blood plasma, stored at specific pH and body temperature conditions [18]. During the test, the material was immersed in SBF that simulates the organic part of blood plasma without cell culture.

Research showed that the results of hydroxyapatite-gelatin composition variation viscosity 45:55, 50:50 and 55:45 were  $(38.7 \pm 0.53)$  dPa.s,  $(49.6 \pm 1.02)$  dPa.s, and  $(66 \pm 1)$  dPa.s, respectively. The pH was around 7 to 7.9 for resuspension test of hydroxyapatite-gelatin based IBS suspension with addition of alendronate before mixing with SBF, after mixing, and after sedimentation. The scaffold that needed 5-6 hours for setting and hardening process, was immersed in IBS suspension for an hour and was dried at room temperature. And the change in scaffold mass increased from 0.12 gram to 0.26 gram in wet condition and 0.21 gram in dry condition. The degradation test in vitro of IBS infusing in the scaffold, conducted with several test. Some of them are molecular weight change, scaffold weight loss, and measuring the mechanical properties of scaffolds [13], [19], [20]. However, that test needs more effort, especially at real time monitoring weight change and weight loss of IBS.

In this study, degradation testing of IBS-paste-infused scaffolds was conducted using Electrical Impedance Spectroscopy (EIS) to obtain electrical impedance spectra in real time and analyze them. EIS is a method for analyzing the electrical properties of materials and systems by inducing alternating current signals and measuring the potential signals as responses [21]. Each material has its characteristic impedance because different materials have varying electrical conductivity abilities, one of them are tissues [22], [23].

The aim of this research is to analyze the degradation results of IBS-paste-infused scaffolds as drug delivery systems using the EIS method. Several characterizations were required, including UV-Vis analysis to determine the streptomycin content in the degradation solution at different time intervals and

morphological examination using a Digital Microscope to observe changes in pore size in scaffolds with IBS paste.

## 2.0 METHODOLOGY

The procedures carried out in this research included the creation of 3D-printed scaffolds and IBS paste, which was then injected into the scaffold. The IBS-added scaffold was let to dry in room temperature for about 5-6 hours. Subsequently, the IBS-added scaffold was characterized by several tests, including its degradation profile with SBF (Simulated Body Fluid) solution, its morphology using a digital microscope, UV-Vis test, and Electrical Impedance Spectroscopy (EIS) test. Furthermore, a comparison was made between the degradation test running by UV-Vis and EIS.

The scaffold was shaped like a truncated hexahedron with a pore size designed at 600  $\mu\text{m}$ , based on a study [24], which claimed that a 600  $\mu\text{m}$  pore size resulted in maximum bone growth capacity. Furthermore, according to research conducted by Yuliatin [20], this pore size exhibited good mechanical properties. Sample printing was carried out using a 3D printer employing FDM (Fused Deposition Modeling) with PLA (poly Lactic Acid) as the raw material filament, heated to its melting point to make the material semi-solid.

The creation of IBS refers to research conducted by Maulida [25]. IBS paste was made from hydroxyapatite (HA) as the main ingredient, gelatin, HPMC, and streptomycin. The initial stage of the paste-making process began with dissolving 20% w/v gelatin in distilled water at a temperature of 40°C for one hour. After that, HPMC was dissolved with a 4% w/v concentration in distilled water at a temperature of 90°C for one hour, which was then cooled down until 40°C. Subsequently, HA powder was added to the gelatin solution with a 65:35 w/w ratio of HA to gelatin, which was stirred for 1 hour. After the solution became homogeneous, the next step was adding 10% streptomycin from the total mass of HA, gelatin, and HPMC, and dissolving it again until the solution became homogeneous. Next, add the HPMC solution to the well-mixed HA, gelatin, streptomycin solution at a temperature of 40°C for 6 hours.

The process of integrating the IBS paste with the 3D-printed scaffold was done by injecting the IBS paste into the scaffold and letting it set to dry and hardened for 5-6 hours. Degradation tests on the ability of scaffolds with IBS paste *in vitro* were carried out using an SBF solution. Simulated Body Fluid (SBF) is an acellular calcium-phosphate solution, protein-free, with composition and ionic concentration almost identical to human blood plasma, and it generally persists under physiological conditions (pH 7.4 and 36.5°C) [26].

During the degradation test, the sample was immersed in a synthetic solution that simulates the

inorganic part of the blood plasma, with or without the presence of cell culture. This method is easy and simple for testing the stability of the sample in the body. The immersion of the sample was conducted in sterile SBF solution at a temperature of 37°C. The reduction in sample weight could be calculated using Equation 1.

$$W_L = \frac{(W_0 - W_1)}{W_0} \times 100\% \quad (1)$$

$W_0$  represented the weight of the sample before the immersion,  $W_1$  was the weight after immersion, and  $W_L$  was the decrease of IBS-integrated scaffold [27]. The morphological test using a Digital Microscope aimed to determine the pore size in the scaffold injected with IBS paste. In the analysis process, the image was analyzed with the ImageJ application.

The UV-Vis test aimed to identify the absorbance value and the percentage of streptomycin concentration lost or the amount of IBS paste scaffold that was degraded. To determine the concentration percentage of the released streptomycin, various concentrations of it were run using UV-Vis. The absorbance data obtained were then plotted into a graph of the relationship between absorbance and concentration. Therefore, a linear regression equation could be obtained. This linear standard curve then becomes a reference for determining the concentration of degraded IBS in the sample with unidentified level of degradations.

The EIS test aimed to identify impedance spectroscopy in the sample being tested. This EIS test used a set of Electrical Impedance Spectroscopy tools. The output results obtained by the EIS device for the test sample were in the form of a graph of the relationship between real Z and Imaginary Z. The first step was testing the IBS paste scaffold before immersing it in the SBF solution to determine the impedance of the sample by attaching gel electrodes at 2 points of the IBS paste scaffold. Subsequently, after the degradation test using SBF solution, it was tested again using EIS with one of the methods to identify impedance in the sample. The first curve obtained is the comparison of Z magnitude ( $|Z|$ ) with frequency ( $\omega$ ), and the second curve is the comparison of phase ( $\theta$ ) with frequency ( $\omega$ ), which is called a bode plot. From this curve, we get a Nyquist graph of the relationship between Imaginary Z and real Z.

## 3.0 RESULTS AND DISCUSSION

The scaffold was designed in the shape of a truncated hexahedron using the Solidworks program, and 3D printing used the FDM technique with PLA as the base material to produce a PLA scaffold with a pore size of 800  $\mu\text{m}$ , as shown in Figure 1(a). Although previous studies have suggested that a pore size of approximately 600  $\mu\text{m}$  is optimal for promoting bone growth [24], the scaffold developed in this study was

designed with a slightly larger initial pore size of 800  $\mu\text{m}$ . This adjustment accounts for the subsequent injection of IBS paste into the scaffold, which would be expected to reduce the effective pore size once it was set.

IBS paste was made in a 65:35 ratio of HA: gelatin, based on research by Maulida [25] that showed favorable properties of homogeneity and well-injectable. The composition of this IBS paste included hydroxyapatite, gelatin, HPMC, and streptomycin. The IBS paste was then injected into the 3D-printed scaffold. The process of injecting IBS paste into the scaffold involved dipping the IBS paste and injecting it with a needle diameter of 0.5 mm evenly into the pores. The results of the injection were left for 24 hours at room temperature, as shown in Figure 1(b).

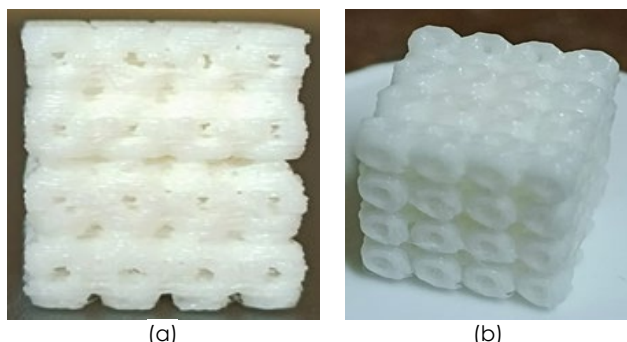


**Figure 1** (a) 3D-printed scaffold 800  $\mu\text{m}$  pore size (b) Scaffold which had been injected with IBS paste

The mass of IBS paste that fills the pore space of the PLA scaffold was determined by finding the difference in the mass of the scaffold before and after the paste injection. The IBS paste mass mean data from the samples with 5-time repetitions was  $0.2525 \pm 0.0030$  grams, and each mass is shown in Figure 2.

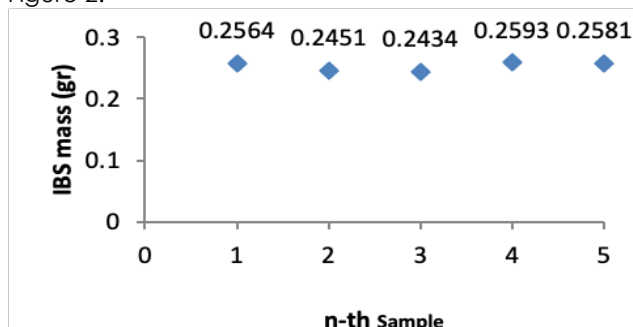
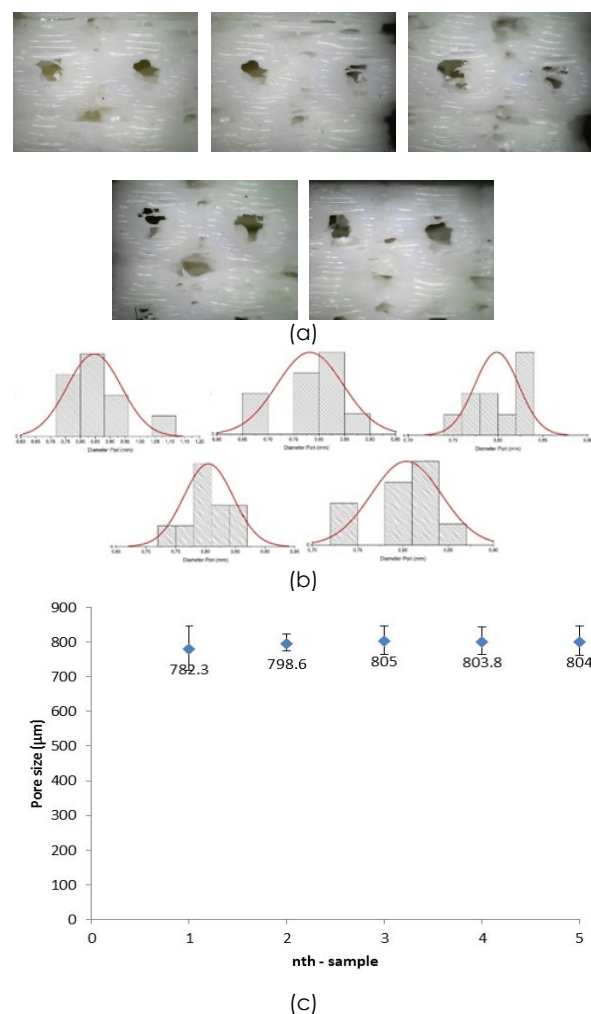


**Figure 2** The relationship between the n-th sample and the mass of paste that has been injected

Figure 2 shows that the pore size of 800  $\mu\text{m}$ , which has been injected with IBS paste, has a relatively similar mass, as evidenced by the very small standard deviation, namely 1.2%.

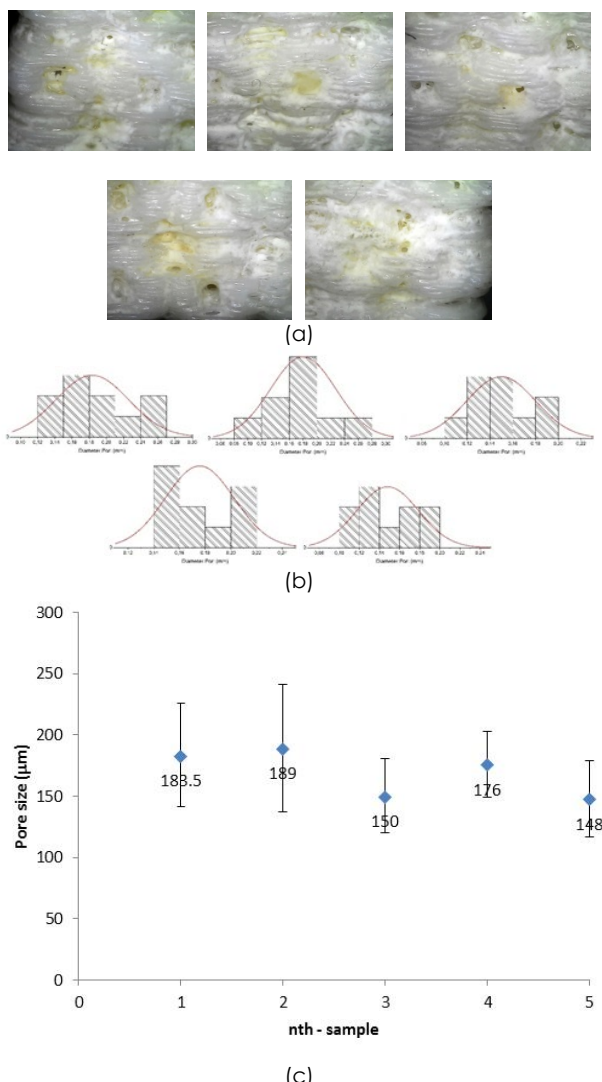
Scaffold pores were measured both before the injection of IBS paste and after degradation. Ten different pores from each of the scaffolds were

selected and measured, as shown in Figures 3(a)(b)(c), 4(a)(b)(c), and 5(a)(b)(c).



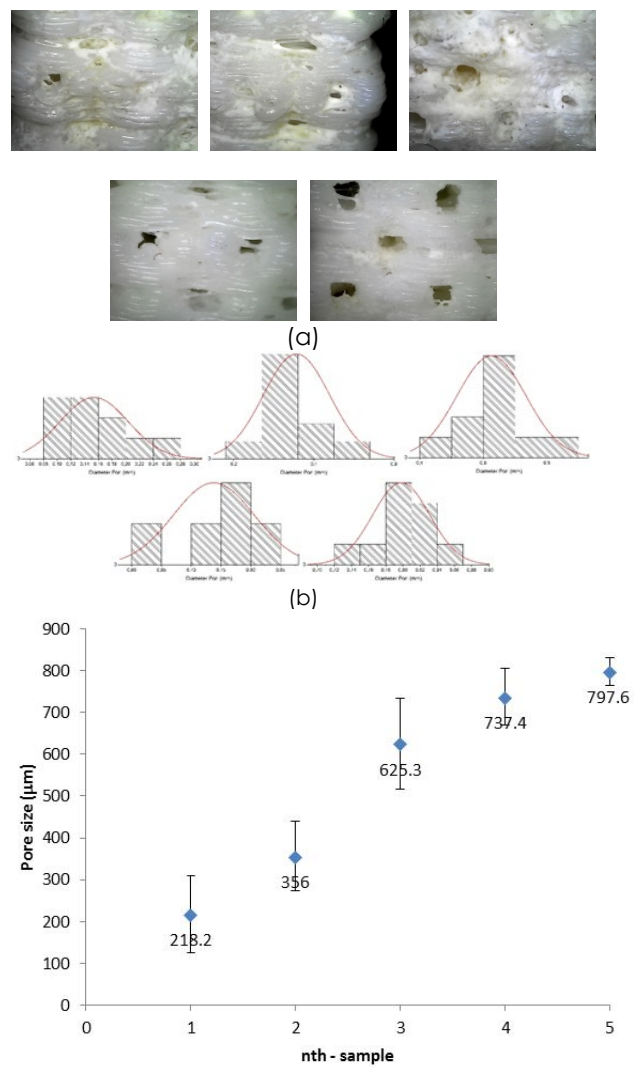
**Figure 3** Scaffold IBS before paste injection (a) Scaffold appearance captured by microscope (b) Pore size distribution of scaffold (c) Pore size of the scaffold

Figure 4 shows that the white colored surface of the sample is the IBS paste. Macroscopically, it can be seen that all pores have been covered by the IBS paste. Scaffolds that have been injected with IBS paste show pores ranging from 148  $\mu\text{m}$  to 183  $\mu\text{m}$ . These pore sizes fulfil the micropore criteria of scaffolds as bone substitutes. Pore sizes greater than 100  $\mu\text{m}$  and less than 400  $\mu\text{m}$  are considered ideal for osteoconduction [29]. Based on the pore size results, it shows that the scaffold has fulfilled the criteria in the process of new bone growth and for cell nutrition.



**Figure 4** Scaffold IBS after paste injection (a) Scaffold's appearance captured by microscope (b) Pore size distribution of scaffold (c) Pore size of scaffold

A degradation test was carried out to determine the extent of degradation experienced by the IBS paste scaffold, which plays a role in the formation of new bone and serves as a drug carrier. Degradation testing of the IBS paste-integrated scaffold was conducted periodically and in a controlled manner by immersing the samples in SBF solution for 5 weeks. The results of the degradation test were expressed as the degradation percentage of the IBS paste injected into the scaffold, using Equation (1). The percentage degradation results obtained are shown in Figure 6, displaying the relationship between pore size and the percentage of scaffold that was degraded every week. It is known that in the length of 5 week, the mass loss reached 15.17%



**Figure 5** Scaffold after one-week degradation (a) Scaffold's appearance captured by microscope (b) Pore size distribution of scaffold (c) Pore size of scaffold

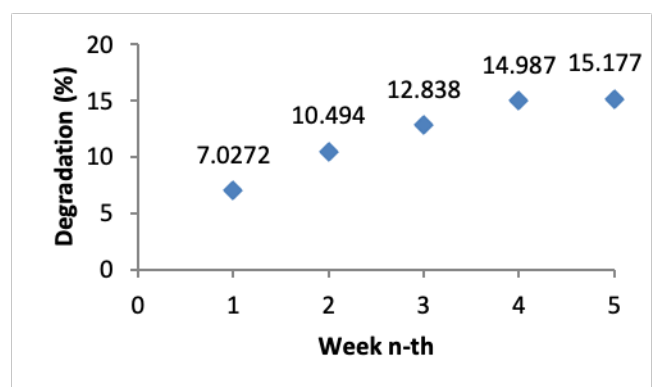


**Figure 6** Degradation percentage of IBS integrated scaffold each week

Figure 6 illustrates that the IBS paste mass degraded in the scaffold samples from week 1 to week 5. The decrease in sample mass was influenced by the length of soaking in the SBF solution.

Hydroxyapatite plays a role in the process of forming an apatite layer, serving as proof that the scaffold material possesses bioactive properties.  By week 5, it was observed that the IBS-pasted scaffold was almost completely degraded. Since this treatment is intended to help and improve the efficacy of the initial bone transplant technique, a five-week release time is deemed adequate, guaranteeing continued support during the crucial early phases of healing and integration of the diseased bone. In this degradation process, it could be observed that the degraded IBS paste scaffold releases streptomycin, making it act as a drug carrier. To determine the amount of streptomycin released, a UV-Vis test was carried out.

The UV-Vis test was conducted to determine the concentration of IBS paste released over a period of 1 week to 5 weeks. Before testing the scaffold with IBS paste, a calibration standard curve was created first to determine the correlation between IBS paste concentration and absorbance using a UV-Vis spectrophotometer. The concentrations of IBS paste used ranged from 1% to 5%. This variation of IBS paste was created by dissolving 0.1 g to 0.5 g of IBS paste in 10 ml of SBF solution. Based on the test results, absorbance data were obtained from several solution concentrations, as shown in Figure 7.

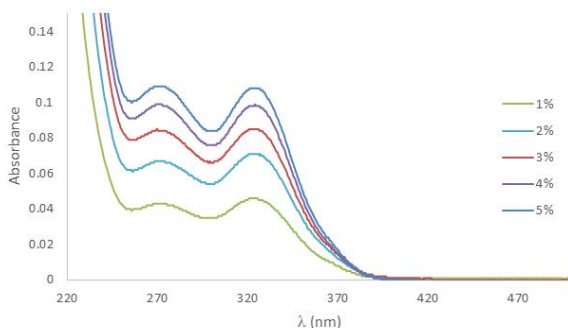


Figure 7 UV-Vis absorbance for calibration solution

Based on Figure 7, there are two absorbance peaks at wavelengths 269 nm - 273 nm and 322 nm - 324 nm. Referring to research by Yuliatin [20], the peak absorbance of streptomycin is at a wavelength of 322 nm - 324 nm. The results of the correlation standard curve between absorbance and the concentration of the IBS paste solution can be seen in Figure 8, which shows a linear curve with a correlation of  $R^2 = 0.9664$ . The linear equation for the relationship between absorbance and concentration of a standard solution is expressed by Equation (2).

$$y = 1.52x + 0.0362 \quad (2)$$

The UV-Vis result for the degradation test of the 5 scaffold samples with different immersion times is shown in Figure 8.

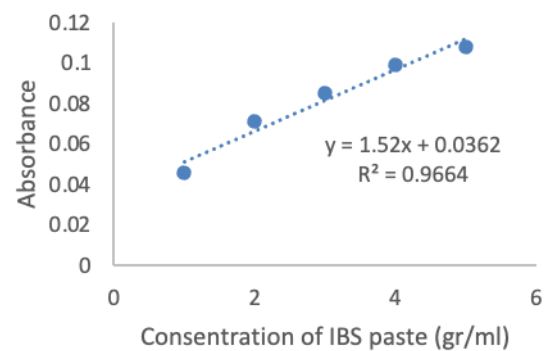


Figure 8 Standard curve of IBS paste concentration

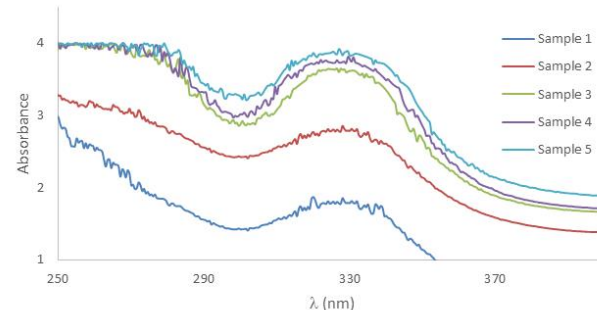


Figure 9 UV-Vis absorbance for the released streptomycin

The absorbance results at each time variation were then substituted into equation (2) to obtain the concentration value of the released IBS paste. The variation of scaffold immersion time on the concentration of IBS paste released is shown in Figure 10. These results represent the concentration of IBS paste released in 10 ml of SBF solution.

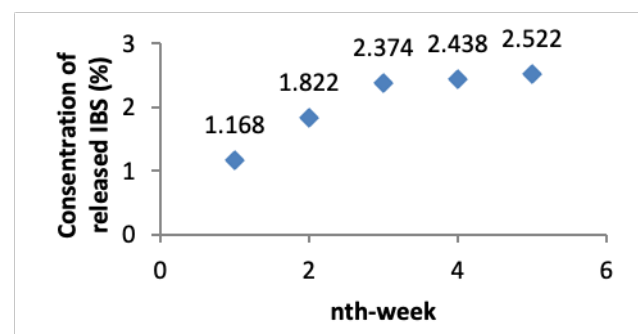
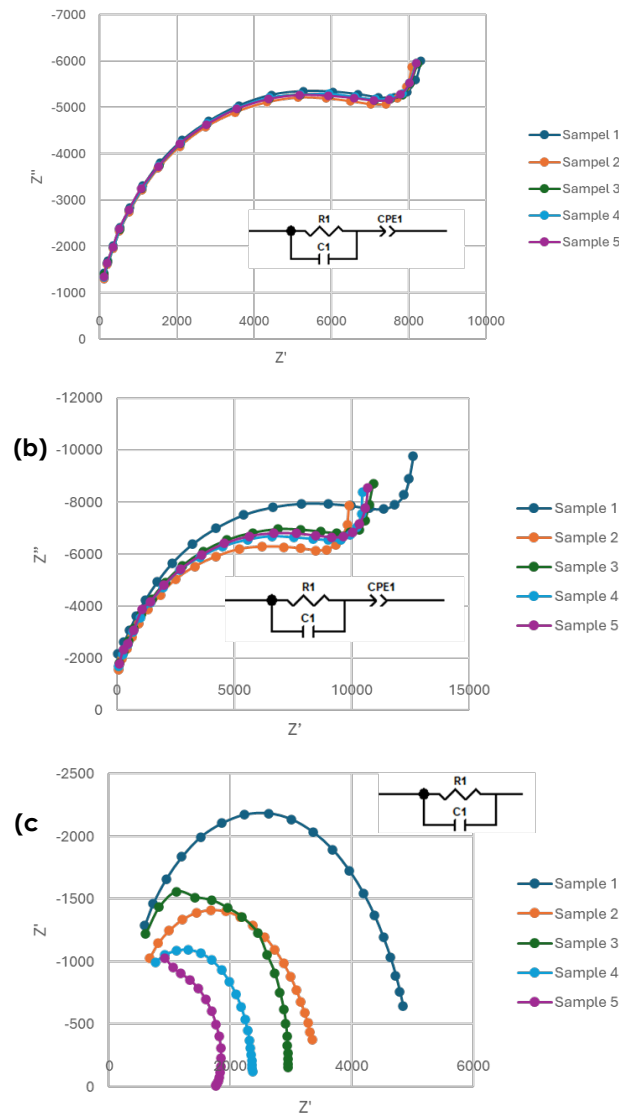


Figure 10 Released IBS Paste Concentration Test Results

Based on the graphic results, a positive correlation between time variations and concentration values was obtained. The smallest percentage of loose IBS paste concentration occurred in week 1, namely 2.337%, and the largest in week 5, amounting to 5.045%. This indicates that the longer the scaffold is degraded, the more IBS paste will be released, showing that the scaffold can play a role in the

process of releasing the drug streptomycin as a treatment for tuberculosis.

The Electrical Impedance Spectroscopy test was carried out on scaffolds. Scaffolds that had been injected with IBS paste and subjected to a degradation test, each Nyquist plot spectrum was shown in Figure 11. The EIS test resulted in Nyquist plot data, which was then fitted with the help of the Z-view application to find the component values composing impedance ( $Z$ ). The Nyquist plot is a graph that lays out the impedance and phase values measured in a certain frequency range. In this study, the frequencies used were 5 kHz to 25 MHz.



**Figure 11** Nyquist plot EIS of (a) scaffold, (b) scaffold that had been injected with IBS (c) scaffold that had been gone through degradation test

From testing using EIS, the circuit model chosen for the scaffold and scaffold injected with IBS paste was a parallel RC in series with CPE. Meanwhile, for the scaffolds that had undergone the degradation test,

a parallel RC circuit model was selected, as shown in Figure 11. The results of fitting each Nyquist plot of the impedance parameters data are shown in Tables 1, 2, and 3.

**Table 1** The impedance parameters data of the scaffold before IBS paste injection

Sampel	R1 (Ω)	C1 (F)	CPE1-T	CPE1-P
1	8542	5.006E-12	5.982E-11	0.985780
2	8623	4.944E-12	6.076E-11	0.984370
3	8379	5.193E-12	6.005E-11	0.986960
4	8510	5.042E-12	6.025E-11	0.985730
5	8547	5.107E-12	5.799E-11	0.988400
Σ	8520,2	5.058E-12	5.9774E-11	0.986248
σ	89.167	9.563E-14	1.0559E-12	0.00151264
% error	0.0104%	0.0189%	0.0176%	0.0015%

The parallel RC circuit model in series with the CPE on the scaffold was chosen because a semicircular pattern was obtained from the parallel R//C circuit, and the depression factor correction was carried out by entering a CPE factor with a value of  $a = 0$  to  $1$ . The convergence error percentage obtained was no more than 5%, indicating that the value of each component  $R$ ,  $C$ , CPE-T, and CPE-P from the model had been sufficiently accurate.

Figure 11(b) displays the impedance resulting from the injection of IBS paste into the scaffold, which has the same behavior as the scaffold. Therefore, the model used was the same, a parallel RC circuit in series with the CPE.

**Table 2** The impedance parameters data in the scaffold after IBS paste injection

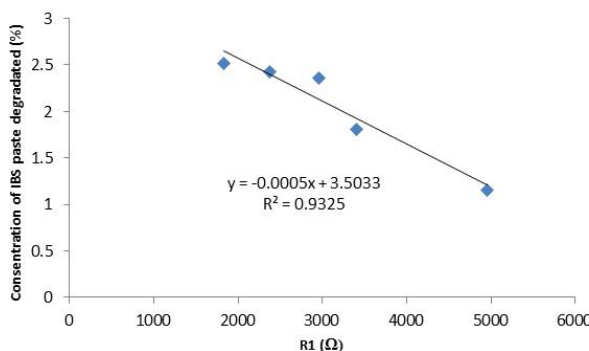
Sampel	R1 (Ω)	C1 (F)	CPE1-T	CPE1-P
1	11184.00	3.417E-12	8.956E-11	0.93090
2	11658.00	3.380E-12	6.086E-11	0.95705
3	10239.00	3.887E-12	6.682E-11	0.95887
4	9876.00	4.082E-12	6.731E-11	0.96236
5	10493.00	3.991E-12	5.180E-11	0.97921
Σ	10690.00	3.751E-12	6.721E-11	0.95767
σ	722.12	3.297E-13	1.394E-11	0.01735
% error	0.0675%	0.0878%	0.2074%	0.0181%

Table 2 shows an increase in the  $R$ -value after the injection of IBS paste, compared to the  $R$ -value in Table 1 before the injection. This indicates that the injected IBS paste was successfully detected through the EIS spectrum. Table 3 shows that the degradation test from week 1 to week 5 resulted in a constant decrease in the  $R$ -value using the parallel RC circuit model. It is assumed that the electrical circuit elements that contribute, consisting of  $R$  and  $C$ , are resistance (which inhibits current flow) and capacitance (which causes charge polarization) [31]. This is illustrated in Table 3, where the  $R$ -value decreased every week.

**Table 3** The impedance parameters data in the scaffold after degraded using 2<sup>nd</sup> model

Sampel	R1 (Ω)	C1 (F)
1	4953	5.19E-12
2	3410	6.123E-12
3	2957	3.718E-12
4	2372	4.422E-12
5	1835	1.752E-12

If a relationship curve is created between Table 3 (R1 or C1 value) and Figure 9 and equation (2) (released IBS paste concentration), a relationship will be obtained between R1 or C1 and the released IBS paste concentration, as shown in Figures 12 and 13.



**Figure 13** Correlation of IBS paste and R1 scaffold concentrations after degradation test

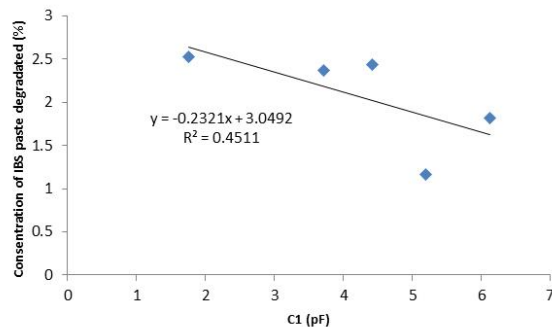


**Figure 14** Correlation of IBS paste and C1 scaffold concentrations after degradation test

From Figures 13 and 14, it can be seen that a correlation curve was obtained between the concentration of degraded IBS paste to R1 and C1 from the electrical impedance spectrum of the scaffold. In Figure 12, R1 has negative slope with a correlation of  $R^2 = 0.9325$ . Likewise, in Figure 13, C1 also has negative slope with a value of  $R^2 = 0.4511$ . The graph shows that the more absorbance obtained from the degradation results, the more the value of the resistor (R) will decrease. Moreover, the more the absorbance value, the more the value of the capacitor (C) will decrease because the resistance on the scaffold decreases during degradation from week 1 to week 5.

The results demonstrate that EIS has significant potential for real-time monitoring of scaffold-induced weight loss. Moreover, with further investigation, this technology shows promise for real-time assessment of drug release, even after the bone scaffold is implanted *in vivo*. This potential has been supported by a study indicating that EIS can effectively detect bone porosity and mechanical properties, which are critical for preventing osteoporosis [30].

## 4 CONCLUSION

The degradation profile of IBS paste, which is injected into a bone scaffold for treating tuberculosis in bone tissue, is a critical factor to study. This is because the embedded drug is released as the paste degrades. This study investigates the potential of electrochemical impedance spectroscopy (EIS) to assess the degradation of IBS-integrated bone scaffolds. The findings were validated by comparing impedance results with UV-Vis absorbance measurements obtained during the material's degradation process. Over a five-week period, UV-Vis analysis showed a progressive increase in the concentration of released IBS paste, ranging from 1.168% at week 1 to 2.522% at week 5. Considering that this treatment is designed to enhance the efficacy of initial bone transplantation techniques, a release duration of five weeks is considered sufficient to provide continued therapeutic support during the critical early stages of bone healing and integration. Furthermore, EIS analysis using an RC parallel circuit model demonstrated a correlation with  $R^2=0.9325$  for the resistance (R) parameter and  $R^2=0.4511$  for the capacitance (C) parameter after degradation.

## Acknowledgement

This work was supported by The Directorate General of Higher Education, Research, and Technology (DRTPM) 2023 under Decree No. 0536/E5/PG.02.00/2023 and Contract No. 114/E5/PG.02.00.PL/2023; 1299/UN3.LPPM/PT.01.03/2023.

## Conflicts of Interest

All authors declare that they have no conflicts of interest.

## References

- [1] World Health Organization (WHO). 2022. *Global Tuberculosis Report 2022*. Geneva: World Health Organization.
- [2] Tarmizi, Siti Nurhaliza. 2023. Deteksi TBC Capai Rekor Tertinggi di Tahun 2022. *Sehat Negeriku*. March 31, 2023. <https://sehatnegeriku.kemkes.go.id/baca/rlis->

- [3] media/20230331/3942688/deteksi-tbc-capai-rekor-tertinggi-di-tahun-2022/.
- [4] Smith, Ian. 2003. *Mycobacterium tuberculosis Pathogenesis and Molecular Determinants of Virulence*. *Clinical Microbiology Reviews*. 16(3): 463–496. <https://doi.org/10.1128/CMR.16.3.463-496.2003>.
- [5] Garg, Ravindra K., and Devendra S. Somvanshi. 2011. *Spinal Tuberculosis: A Review*. *Journal of Spinal Cord Medicine*. 34(5): 440–454. <https://doi.org/10.1179/2045772311Y.0000000023>.
- [6] Kalanjati, Valentina P., Rizki T. Oktariza, Yoyos Yahya, and Ahmad Machin. 2020. *Paralytic Ileus in the Patient with Tuberculosis of Spine*. *British Journal of Neurosurgery*. 34(6): 602–603. <https://doi.org/10.1080/02688697.2019.1639621>.
- [7] Inzana, Jason A., Edward M. Schwarz, Stephen L. Kates, and Hani A. Awad. 2016. *Biomaterials Approaches to Treating Implant-Associated Osteomyelitis*. *Biomaterials*. 81: 58–71. <https://doi.org/10.1016/j.biomaterials.2015.12.012>.
- [8] Paiva, João C. C., Luís Oliveira, Maria F. Vaz, and Sofia Costa-de-Oliveira. 2022. *Biodegradable Bone Implants as a New Hope to Reduce Device-Associated Infections: A Systematic Review*. *Bioengineering*. 9(8): 409. <https://doi.org/10.3390/bioengineering9080409>.
- [9] Florencio-Silva, Rodrigo, Gustavo R. da S. Sasso, Eliana Sasso-Cerri, Maria J. Simões, and Paulo S. Cerri. 2015. *Biology of Bone Tissue: Structure, Function, and Factors That Influence Bone Cells*. *BioMed Research International*. 2015: 1–17. <https://doi.org/10.1155/2015/421746>.
- [10] Feng, Peng, Jian Jia, Meng Liu, Shuping Peng, Zhen Zhao, and Chengde Shuai. 2021. *Degradation Mechanisms and Acceleration Strategies of Poly (Lactic Acid) Scaffold for Bone Regeneration*. *Materials & Design*. 210: 110066. <https://doi.org/10.1016/j.matdes.2021.110066>.
- [11] Polo-Corrales, Lorena, Maribel Latorre-Esteves, and Juan E. Ramirez-Vick. 2014. *Scaffold Design for Bone Regeneration*. *Journal of Nanoscience and Nanotechnology*. 14(1): 15–56. <https://doi.org/10.1166/jnn.2014.9127>.
- [12] Roosa, S. M. M., J. M. Kemppainen, E. N. Moffitt, P. H. Krebsbach, and S. J. Hollister. 2010. *The Pore Size of Polycaprolactone Scaffolds Has Limited Influence on Bone Regeneration in an In Vivo Model*. *Journal of Biomedical Materials Research Part A*. 92A(1): 359–368. <https://doi.org/10.1002/jbm.a.32381>.
- [13] Larsson, S., and G. Hannink. 2011. *Injectable Bone-Graft Substitutes: Current Products, Their Characteristics and Indications, and New Developments*. *Injury*. 42(Suppl. 2): S30–S34. <https://doi.org/10.1016/j.injury.2011.06.013>.
- [14] Putra, A. P., D. Hikmawati, and A. S. Budiatin. 2019. *Injectable Bone Substitute of Hydroxyapatite–Gelatin Composite with Alendronate for Bone Defect Due to Osteoporosis*. Accessed via Semantic Scholar. <https://api.semanticscholar.org/CorpusID:199368287>.
- [15] Moussi, H., P. Weiss, J. Le Bideau, H. Gautier, and B. Charbonnier. 2022. *Injectable Macromolecule-Based Calcium Phosphate Bone Substitutes*. *Materials Advances*. 3(15): 6125–6141. <https://doi.org/10.1039/D2MA00410K>.
- [16] Bongio, M., J. J. J. P. van den Beucken, S. C. G. Leeuwenburgh, and J. A. Jansen. 2015. *Preclinical Evaluation of Injectable Bone Substitute Materials*. *Journal of Tissue Engineering and Regenerative Medicine*. 9(3): 191–209. <https://doi.org/10.1002/term.1637>.
- [17] Fellah, B. H., P. Weiss, O. Gauthier, T. Rouillon, P. Pilet, G. Daculsi, and P. Layrolle. 2006. *Bone Repair Using a New Injectable Self-Crosslinkable Bone Substitute*. *Journal of Orthopaedic Research*. 24(4): 628–635. <https://doi.org/10.1002/jor.20125>.
- [18] Nilsson, M., E. Fernández, J. A. Planell, I. McCarthy, and L. Lidgren. 2003. *The Effect of Aging an Injectable Bone Graft Substitute in Simulated Body Fluid*. *Key Engineering Materials*. 240–242: 403–406. <https://doi.org/10.4028/www.scientific.net/KEM.240-242.403>.
- [19] Yilmaz, B., A. E. Pazarceviren, A. Tezcaner, and Z. Evis. 2020. *Historical Development of Simulated Body Fluids Used in Biomedical Applications: A Review*. *Microchemical Journal*. 155: 104713. <https://doi.org/10.1016/j.microc.2020.104713>.
- [20] Jiang, T., S. P. Nukavarapu, M. Deng, E. Jabbarzadeh, M. D. Kofron, S. B. Doty, W. I. Abdel-Fattah, and C. T. Laurencin. 2010. *Chitosan–Poly(lactide-co-glycolide) Microsphere-Based Scaffolds for Bone Tissue Engineering: In Vitro Degradation and In Vivo Bone Regeneration Studies*. *Acta Biomaterialia*. 6(9): 3457–3470. <https://doi.org/10.1016/j.actbio.2010.03.023>.
- [21] Yuliatin, E., D. Hikmawati, A. Aminatun, A. S. Budiatin, P. Widiyanti, and F. Parastuti. 2023. *Tensile Strength of 3D Printing Scaffold Design Truncated Hexahedron for Tuberculosis Drug Delivery*. *Engineering Innovations*. 4: 31–36. <https://doi.org/10.4028/p-4wu1vu>.
- [22] Ain, K., A. P. Putra, O. N. Rahma, D. Hikmawati, A. Rahmatullah, and C. A. C. Abdullah. 2022. *Electrical Impedance Spectroscopy as a Potential Tool for Detecting Bone Porosity*. *SSRN Electronic Journal*. <https://doi.org/10.2139/ssrn.4111257>.
- [23] Bertemes-Filho, P. 2018. *Electrical Impedance Spectroscopy*. In *Bioimpedance in Biomedical Applications and Research*. 5–27. Springer International Publishing. [https://doi.org/10.1007/978-3-319-74388-2\\_2](https://doi.org/10.1007/978-3-319-74388-2_2).
- [24] Dean, D. A., T. Ramanathan, D. Machado, and R. Sundararajan. 2008. *Electrical Impedance Spectroscopy Study of Biological Tissues*. *Journal of Electrostatics*. 66(3–4): 165–177. <https://doi.org/10.1016/j.elstat.2007.11.005>.
- [25] Taniguchi, N., S. Fujibayashi, M. Takemoto, K. Sasaki, B. Otsuki, T. Nakamura, T. Matsushita, T. Kokubo, and S. Matsuda. 2016. *Effect of Pore Size on Bone Ingrowth into Porous Titanium Implants Fabricated by Additive Manufacturing: An In Vivo Experiment*. *Materials Science and Engineering: C*. 59: 690–701. <https://doi.org/10.1016/j.msec.2015.10.069>.
- [26] Nur Maulida, H., D. Hikmawati, and A. S. Budiatin. 2015. *Injectable Bone Substitute Paste Based on Hydroxyapatite, Gelatin and Streptomycin for Spinal Tuberculosis*. *Journal of Spine*. 4(6). <https://doi.org/10.4172/2165-7939.1000266>.
- [27] Hikmawati, D., H. N. Maulida, A. P. Putra, A. S. Budiatin, and A. Syahrom. 2019. *Synthesis and Characterization of Nanohydroxyapatite–Gelatin Composite with Streptomycin as Antituberculosis Injectable Bone Substitute*. *International Journal of Biomaterials*. 2019: 1–8. <https://doi.org/10.1155/2019/7179243>.
- [28] Venkatesan, S. 2012. *Stamp Forming of Composite Materials: An Experimental and Analytical Study*. Australian National University. <https://doi.org/10.25911/5d5142259ddd4>.
- [29] Hutmacher, D. W. 2000. *Scaffolds in Tissue Engineering Bone and Cartilage*. *Biomaterials*. 21(24): 2529–2543. [https://doi.org/10.1016/S0142-9612\(00\)00121-6](https://doi.org/10.1016/S0142-9612(00)00121-6).
- [30] Roosa, S. M. M., J. M. Kemppainen, E. N. Moffitt, P. H. Krebsbach, and S. J. Hollister. 2010. *The Pore Size of Polycaprolactone Scaffolds Has Limited Influence on Bone Regeneration in an In Vivo Model*. *Journal of Biomedical Materials Research Part A*. 92A(1): 359–368. <https://doi.org/10.1002/jbm.a.32381>.
- [31] Ain, K., A. P. Putra, O. N. Rahma, D. Hikmawati, A. Rahmatullah, and C. A. C. Abdullah. 2024. *Electrical Impedance Spectroscopy as a Potential Tool for Detecting Bone Porosity*. *Sensors and Actuators A: Physical*. 370: 115252. <https://doi.org/10.1016/j.sna.2024.115252>.
- [32] Syahril. 2012. *Studi Spektroskopi Impedansi Barium Titanat Pada Temperatur Tinggi*. Master's thesis, Universitas Indonesia.